Odometry during object transport

Alkilabi, Muhanad Hayder Mohammed; Carletti, Timoteo; Tuci, Elio

Published in:
Advances in Swarm Intelligence - 12th International Conference, ICSI 2021, Proceedings

DOI:
10.1007/978-3-030-78811-7_9

Publication date:
2021

Odometry during object transport: a study with Swarm of physical robots

Muhanad H.M. Alkilabi
University of Namur, Namur, Belgium
Timoteo Carletti
University of Namur, Namur, Belgium

Elio Tuci
Faculty of Computer Science, University of Namur, Namur, Belgium
elio.tuci@unamur.be

June 14, 2021

Abstract

Object transport by a single robot or by a swarm of robots can be considered a very challenging scenario for odometry since wheel slippage caused by pushing forces exerted on static objects and/or by relatively frequent collisions with other robots (for the cooperative transport case) tend to undermine the precision of the position and orientation estimates. This paper describes two sets of experiments aimed at evaluating the effectiveness of different sensory apparatuses in order to support odometry in autonomous robots engaged in object transport scenarios. In the first set of experiments, a single robot has to track its position while randomly moving in a flat arena with and without an object physically attached to its chassis. In the second set of experiments, a member of a swarm of physical robots is required to track its position while collaborating with the group-mates to the collective transport of a heavy object. In both sets, odometry is performed with either wheel encoders or with an optic-flow sensor. In the second set of experiments, both methods are evaluated with and without gyroscope corrections for angular displacements. The results indicate that odometry based on optic-flow sensors is more precise than the classic odometry based on wheel encoders. In particular, this research suggests that by using an appropriate sensory apparatus (i.e., an optic-flow sensor with gyroscope corrections), odometry can be achieved even in extreme odometry conditions such as those of cooperative object transport scenarios.

1 Introduction

In order to navigate complex environments successfully, autonomous robots may required to keep track of their position with respect to local landmarks or with respect

to a given frame of reference. Compared to single robot systems, multi-robot systems can exploit the collectivity to improve the effectiveness of localisation algorithms. In particular, in distributed localisation algorithms, estimation errors can be reduced by integrating sensor data collected from different agents placed in different positions. The eventual heterogeneity of the system can be exploited to fuse information from different types of sensors [Fox et al., 1999]. The time required for localisation using dynamically built maps (SLAM) can be significantly reduced if different robots explore different parts of the environment simultaneously and subsequently share the information gathered. This process is also referred to as cooperative or collaborative localisation.

Cooperative localisation is achieved by a group of robots exchanging their relative or absolute positions while in close vicinity. In this context, most work on localisation has focused on the question of how to reduce the odometry error using a cooperative team of robots. One way to correct this odometry error is to use apriori defined landmarks which can be detected by the robot's sensors. Unfortunately, detecting and recognising landmarks is a difficult task in general, especially when the environment is much larger than the sensing range of the robot. Alternatively, some studies propose the use of *Mobile Landmarks* based on cooperative localisation [Kurazume et al., 1994]. In such an approach a team of robots is divided into two groups. One group remains stationary and act as landmarks while the other group navigates the environment. The two groups interchange their roles until a target position is reached. The odometry is calculated based on triangular measurements of the distances and the angles between the robots. However, relying on stationary robots will reduce the effectiveness of the group, which are obliged to dedicate a significant amount of their resources to generate landmarks instead of using them to carry out important tasks.

In swarm robotics systems [Dorigo and Şahin, 2004], the generally limited sensory and computational capabilities of the robots make it hard to implement some of the odometry based methods discussed above. To overcome these limitations, several studies rely on approaches that can implement odometry in small size platforms. For example, in [Kernbach, 2012], the author proposes an odometry method for autonomous micro-robots based on the optical properties of a motor-wheel transmission. Such an approach can provide relative localisation for robots where the robot size and its computational resources are limited. In [Vardy, 2016], the author illustrates the ODOCLUST algorithm for an aggregation task. The robots alternate between random motion and odometry guided homing based on the last contact point with other robots to achieve aggregation. The results indicate that the method is robust in coping with odometry errors. In [Gutiérrez et al., 2010], the authors study a swarm robotics foraging scenario where e-puck robots randomly initialised in a bounded arena are required to find a food source and a nest area and then to move back and forth between the two target locations. The authors discuss a navigation and localisation algorithm called *Social Odometry*. Social Odometry is based on peer-to-peer local communication which leads to a self-organised path selection without the need for any central unit.

In this paper, we illustrate and compare the performances of an alternative localisation method for e-puck robots based on the use of an optic-flow sensor and gyroscope for odometry. This method is compared with the classic wheel encoders approach, and it is evaluated in various difference scenarios, such as i) single e-puck randomly mov-

ing in an empty arena; ii) single e-puck randomly moving in an empty arena with an object attached to its chassis; iii) swarms of e-pucks transporting an object that has to be pushed by all the members of the group to be transported . In this scenario, one robot of the swarm is required to track its position. Object transport is a very challenging scenario for odometry since wheel slippage caused by pushing forces exerted on static objects, and by relatively frequent collisions with other robots during the transport, tend to undermine the precision of position and orientation estimates [Tuci et al., 2018]. The results of our study show that the odometry method based on the use of the developed optic-flow sensor which integrated into the e-puck robotics platform combined with gyroscope corrections for angular displacements can significantly reduce the disruptive effects of slippage in both the single robots and the swarm of robots types of scenario.

2 Odometry using single optic-flow sensors

This section describes a method to estimate the robot's changes in position based on the readings of a single optic-flow sensor mounted underneath the e-puck chassis. Optic-flow sensor has been used to improve the coordination among the robots of a swarm required to cooperatively transport heavy objects (as in [Alkilabi et al., 2018, Alkilabi et al., 2017]). The sensor is an optical camera that accurately computes the pixel displacement along x and y components of the robot's translational movements (see Figure1a). The readings of the sensor are delivered in counts format (i.e., *cx* counts in the x-direction and *cy* counts in the y-direction of the robot translational movement). For a detailed description of the characteristics of this sensor see the supplementary material at `https://drive.google.com/file/d/1tZ4kO3PvnSm5EFjQHPdjjWJAP5Qksn55/view?usp=sharing`

The odometry method with the optic-flow sensor is based on the assumption that the robot travels only in the direction orthogonal to the wheel axis. If the kinematic constraints of a differential drive robot are violated due to the external forces (causing the robot to move in the direction of the wheels axis; for the e-puck robot, this is the lateral axis), the method cannot accurately function. In such circumstances, a single optic-flow sensor interprets the lateral motion as a rotation along the robot's centre of mass, rather than a translational movement.

This method, originally proposed in [Lee and Song, 2004], is based on the principle of the relative velocity of a point on a rigid body. According to the kinematics of a rigid body that moves in a two-dimensional space, during translation motion, all points on the body move with the same velocity. In contrast, during rotational motion, all points which lay outside the body's axis of rotation have a different linear velocity. This is due to the fact that their velocity depends on the point's distance from the centre of rotation. All points lying on the rotational axis have zero linear velocity.

Let's assume that this rigid body corresponds to the e-puck body. Point o, whose linear velocity is $\overrightarrow{V_o}$, is at the robot centre of mass, while point s, whose linear velocity is $\overrightarrow{V_s}$, is at a certain distance from o not on the robot's transversal axis. This means that point o has zero linear velocity only when the robot rotates on its transversal axis. $\overrightarrow{\omega}$ is the angular velocity vector of the robot and $\overrightarrow{r}$ is the vector from the position of s to o (see Figure 1b). The cross product $\overrightarrow{\omega} \times \overrightarrow{r}$ refers to the relative velocity of point o

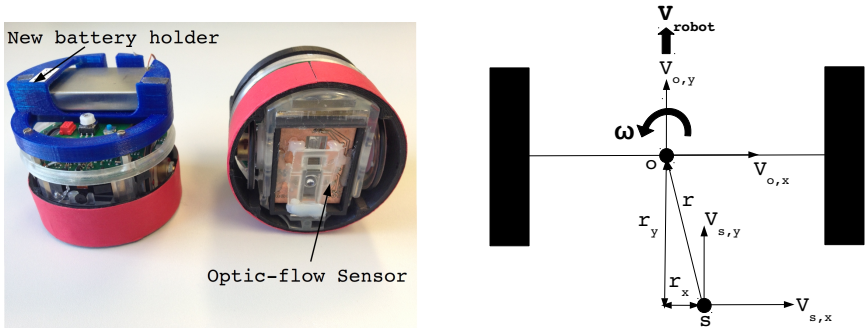

(a) (b)

Figure 1: (a) The optic-flow sensor mounted on the e-puck chassis. (b) Graphs indicating the velocities component of the single optic-flow sensor method to estimate the robot position.

with respect to point s. Providing that the s local frame of reference is aligned with the robot's local frame of reference, the lateral (x) and longitudinal (y) component of the velocity vector of point o, that is $V_{o,x}$ and $V_{o,y}$, can be computed as follows:

$$\overrightarrow{V_o} = \overrightarrow{V_s} + \overrightarrow{\omega} \times \overrightarrow{r}; \qquad V_{o,x} = V_{s,x} - \omega.r_y; \qquad V_{o,y} = V_{s,y} + \omega.r_x; \tag{1}$$

with r_x and r_y being the lateral and longitudinal components of $\overrightarrow{r}$ within the robot local frame of reference (see Figure 1b). Given the kinematics constraints of a differential drive robot like the e-puck, $V_{o,x} = 0$. Given that the linear velocity of the robot is always in the direction orthogonal to the wheels' axis, the linear velocity of point o does not have any lateral component. That is, $V_o = V_{o,y}$. Thus, the angular velocity $\overrightarrow{\omega}$ of the robot and the linear velocity $\overrightarrow{V_o}$ of point o can be computed as follows:

$$\omega = \frac{V_{s,x}}{r_y}; \qquad V_o = V_{s,y} + \frac{r_x}{r_y} V_{s,x}; \tag{2}$$

Assuming the optic-flow sensor is place at s, the velocity at this point can be measured as follows:

$$V_{s,x} = \frac{cx}{R\Delta t}; \qquad V_{s,y} = \frac{cy}{R\Delta t}; \tag{3}$$

where cx and cy are the number of counts returned by the optic-flow sensor for the lateral and longitudinal displacement of point s, and R is the sensor resolution. By sampling the lateral and longitudinal component of the velocity vector of point s using the sensor sampling interval $\Delta t = 50$ ms, it is possible to compute the displacement of point o in the lateral and longitudinal directions.

The change in the robot orientation $\Delta\theta$ and the change in the robot linear displacement Δp (i.e., translational movements) can be computed as follows:

$$\Delta\theta = \frac{cx}{R.r_y}; \quad \Delta p = \frac{cy}{R} + \frac{r_x.cx}{R.r_y}; \tag{4}$$

(a) (b)

Figure 2: (a) E-puck robots with an object attached to its chassis. (b) E-puck with markers for tracking its motion.

Finally, the relative robot position and orientation at time t can be computed as follows:

$$\theta_t = \theta_{t-1} + \Delta\theta; \qquad X_t = X_{t-1} + \Delta p \cos(\theta_t); \qquad Y_t = Y_{t-1} + \Delta p \sin(\theta_t); \tag{5}$$

Odometry using incremental wheel encoders is a common technique to estimate robot changes in position and orientation based on a method called *forward kinematics* which relates the velocity of the robot centre of mass to the velocity of the left and right wheels. As this method is well understood, this section does not describe how these equations are formulated. For a detailed description of the mathematical derivation of forward kinematics equations, see [Borenstein and Feng, 1994] and supplementary material.

3 Results

This section illustrates the results of two sets of experiments aimed at evaluating the effectiveness of different sensory apparatus in order to support odometry in autonomous robots engaged in object transport scenarios. In the first set of experiments (referred to as single-robot condition), a single physical e-puck robot is required to localise itself while randomly exploring a bounded arena both with and without an object physically attached to its chassis (see Figure 2a). In the second set of experiments (referred to as multi-robot condition), a single physical e-puck robot is required to localise itself while transporting with other robots a heavy object in an arbitrarily chosen direction. Both sets of experiments aimed at comparing the effectiveness of an optic-flow sensor based odometry system with a wheel encoders based odometry system.

The results of the single-robot condition test provide evidence of the accuracy of the optic-flow and wheel-encoder based odometry during a relatively simple transport scenario where the object is physically attached to the robot. The dynamics of transport can generate wheel slippage. However, lateral displacements of the robot chassis are unlikely to occur. For both the optic-flow sensor based odometry and the wheel encoders based odometry, the accuracy of the localisation process is compared with a scenario in which the robot moves randomly in a bounded arena without transporting the object. The results of the multi-robot condition provide evidence of the accuracy of the optic-flow and wheel-encoder based odometry in an object transport scenarios where both wheel slippage and lateral displacement of the robot chassis are likely to

happen at any stage of the transport. Comparisons between the odometry performances in single-robot and multi-robot conditions give a quantitative estimate of the disruptive effects on odometry of the phenomena induced by robot-robot and robot-object collisions. In the multi-robot condition, it is shown that the accuracy of the optic-flow and the wheel encoders based odometry can be improved by using the gyroscope sensor for estimating changes in orientation.

In both conditions, the position estimates generated by the robot are compared with the ground truth measured by a Vicon motion capture system. The Vicon system comprises 7 cameras covering the square robot arena (220×220 cm) with a position accuracy of ± 1 mm and orientation accuracy of $\pm 1^{\circ}$. During these tests, a 3D printed square (10×10 cm) with 6 markers is attached on top of the robot as shown in Figure 2b. The aim of this structure is to obtain a better Vicon's accuracy while tracking the position and orientation of the robot during transport.

During all tests, after each update cycle, the robot communicates the estimated change in position Δp and orientation $\Delta\theta$ as calculated by the optic-flow sensor (see eq. 4 in Section 2), and by the wheel encoders to an external computer via Bluetooth. In the multi-robot condition, the robot also communicates the estimated change in orientation as computed by the gyroscope. Along with this information, the external computer records the absolute position of the robot as recorded by the Vicon system and it timestamps the flux of data. The robot trajectories with respect to the Vicon frame of reference are reconstructed offline by the external computer by converting the sequence of local changes in position and orientation into a coherent set of "global" or Vicon based coordinates.

3.1 The single-robot condition

In this condition, a single e-puck robot undergoes 80 trials evaluation. At the beginning of each trial, the robot is placed in the middle of a flat bounded square arena (220×220 cm). During the trial, which last 180 s, the movement of the robot is characterised by an isotropic random walk, with a fixed step length (3 s, at 3.2 cm/s), and turning angles chosen from a wrapped Cauchy probability distribution characterised by the following PDF [Kato and Jones, 2013]:

$$f_{\omega}(\theta,\mu,\rho) = \frac{1}{2\pi}\frac{1-\rho^2}{1+\rho^2-2\rho\cos(\theta-\mu)},\ 0<\rho<1, \tag{6}$$

where $\mu = 0$ is the average value of the distribution, and ρ determines the distribution skewness. For $\rho = 0$ the distribution becomes uniform and provides no correlation between consecutive movements, while for $\rho = 1$ a Dirac distribution is obtained, corresponding to straight-line motion. The robot undergoes 40 trials without object, and 40 trials with an object of 60 g attached to its chassis, as shown in Figure 2a. For both these sets of tests (with and without object), half of the trials (i.e., 20) are with $\rho = 0.3$, and half with $\rho = 0.9$ (video recording of these tests are available at `https://www.youtube.com/embed/HbMRv_nuvm4`).

The results of the single-robot test condition are shown in Figure 3, where white boxes refer the Euclidean distances (in millimetre) between the robot positions at the

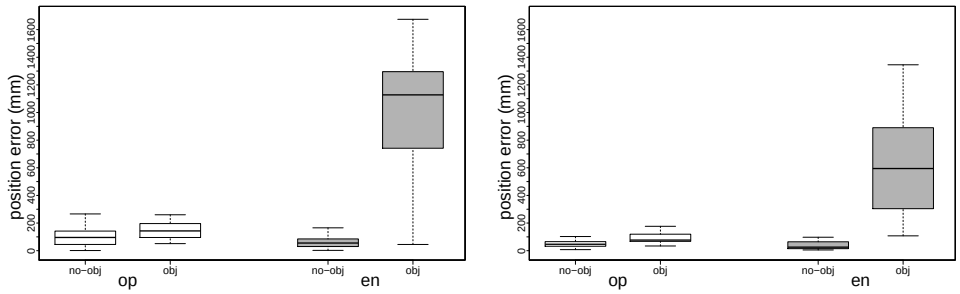

(a) (b)

Figure 3: Graphs showing the position errors for a random walk based on wrapped Cauchy probability distribution with (a) $\rho = 0.3$; (b) $\rho = 0.9$. Position errors correspond to the Euclidean distances (in millimetre) between the final robot's positions recorded by the Vicon (i.e., ground truth) and the estimates of the final robot's positions generated by the optic-flow sensor (white boxes above the "op" x-axis labels) and by the wheels encoder (grey box above the "en" labels). Also on the x-axis, the "no-obj" labels refer to runs without any object attached to the robot chassis, while the "obj" labels refers to runs with an object attached to the robot chassis. Each box is made of 20 points (trials), where each point indicates the position error in a single trial. Boxes represent the inter-quartile range of the data, while horizontal bars inside the boxes mark the median value. The whiskers extend to the most extreme data points within 1.5 times the inter-quartile range from the box.

end of each trial as recorded by the motion caption system and the positions estimated by the optic-flow sensor, for trial without object (see white boxes in correspondence of x-axis label "no-obj"), and for trial with the object attached to the robot chassis (see white boxes in correspondence of x-axis label "obj"). Grey boxes refer to the same distances recorded by the motion caption system and the positions estimated by the wheel encoders, for trials without object (see grey boxes in correspondence of x-axis label "no-obj"), and for trials with the object attached to the robot chassis (see grey boxes in correspondence of x-axis label "obj"). We can clearly notice that in both graphs (differing for the type of random walk, see also Figure caption for details), for those trials with no object attached to the robot ("no-obj" boxes in Figure 3) the median of the position error is less than 10 cm for both the optic-flow sensor estimates, and for the wheels encoder estimates. In those trials where the robot is physically attached to an object, the errors corresponding to the optic flow final position estimates are only slightly higher than the errors recorded in trials with no object (see white boxes in Figure 3). The errors corresponding to the wheel encoder estimates in trials with the object are instead several centimetres higher than the errors registered in the trials without the object (see grey boxes in Figure 3). In trials where the robot has an object attached to it, the median of the position errors corresponding to the estimates generated using the wheels encoders are significantly higher than the errors corresponding to the position

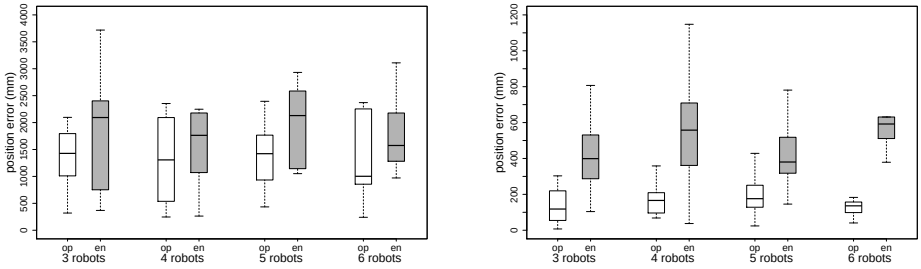

(a) (b)

Figure 4: Graphs showing the position errors referring to the Euclidean distances (in millimetre) between the final *R-robot*'s positions recorded by the Vicon (i.e., ground truth) and the final *R-robot*'s positions estimates generated by: (a) the optic-flow sensor (white boxes above x-axis labels "op") and the wheels encoder (grey boxes, above x-axis labels "en"); (b) the optic-flow sensor with gyroscope corrections (white boxes above x-axis labels "op"), and the wheels encoder with gyroscope corrections (grey boxes above x-axis labels "en"). Tests are run for homogeneous groups of 3, 4, 5, and 6 physical e-puck robots, in 10 trials per group. Each point in the box refers to the position error in a single trial.

estimates generated using the optic-flow sensor (Wilcoxon rank-sum test, $p < 0.001$).

To summarise, without an object attached to the robot chassis, the optic-flow sensor and the wheel encoder generate position estimates quite similar to each other with the median of the position error around 10 cm computed on repeated random walks of 180 s. With an object of 60 g attached to the robot chassis, the optic-flow sensor is a better means to generate position estimates than the wheel encoder. The wheel slippage events disrupt only the wheels encoder estimates.

3.2 The multi-robot condition

This section describes the results of a further series of experiments in which homogeneous groups of 3, 4, 5 and 6 robots are required to push a cuboid object as far as possible from its initial position in an arbitrary direction. The robots are controlled by dynamic neural networks shaped using evolutionary robotics approach. In each group, there is a robot, referred to as *R-robot*, whose position is estimated using both the readings of its optic-flow sensor and its wheel encoders. The accuracy of the optic-flow and the wheel encoder based odometry of the *R-robot* are evaluated with respect to the ground truth generated by the Vicon. Each group is evaluated for 10 trials. In each of these 10 trials i) the *R-robot* is involved in the transport for the entire duration of the trial; ii) the transport is successful (i.e., the object is transported from its starting position for at least a distance of 1 m. For more details, see video recording of some

trials of this test at https://www.youtube.com/embed/6khzx79OrYc).

In Figure 4a the white boxes refer to the errors corresponding to the position estimates generated with the optic-flows sensor, and the grey boxes refer to the errors corresponding to the position estimates generated with wheel encoders. We can notice that the errors for both types of position estimates are relatively high. Also that errors corresponding to estimates generated by the wheel encoders are slightly higher than the error corresponding to position estimates generated by the optic flow sensor. Generally, wheels slippage occurring at any time while the *R-robot* pushes a static element of the transport scenario—either the cuboid object or another static robot—severely effects the precision of the position estimates generated by wheel encoders. The optic-flow sensor is relatively immune from the consequences of wheel slippage. Unfortunately, in the collective object transport task, wheel slippage events are associated with rather frequent lateral sliding of the robot's body (i.e., robot movements in the direction perpendicular to the wheel direction of rotation), which is a consequence of pushing forces mainly exerted by other robots. Lateral sliding events disrupt the precision of the optic-flow estimates relative to changes of the *R-robot*'s orientation more than they affect the precision of estimates relative to the change in position.

In order to overcome the disruptive effects on odometry associated with the object transport scenario, a further set of tests, were run in which the changes in orientation estimates for both the optic-flow sensor and the wheel encoders are generated using the gyroscope mounted in the *R-robot*. This means that the optic-flow sensor and the wheel encoders are used only to estimate the linear displacements in the two-dimensional navigation space. The results of this set of tests are shown in Figure 4b. We can notice that for both types of final position estimate and for all groups, the errors are much smaller. Moreover, the errors corresponding to the position estimates generated by the optic-flow sensor with gyroscope corrections (see white boxes in Figure 4b) are significantly lower (Wilcoxon rank-sum test, $p < 0.001$) than the errors corresponding to position estimates generated by the wheel encoders with gyroscope (see white boxes in Figure 4b). We conclude that in this cooperative object transport scenario, the optic-flow sensor with gyroscope correction results in a better means for odometry than the wheel encoder with gyroscope correction. The optic-flow generates fairly accurate position estimation compared to the wheel encoder. The latter method generates position estimates characterised by trajectory lengths longer than those of the actual trajectory (see the trajectory graphs described in supplementary material at https://drive.google.com/file/d/1tZ4kO3PvnSm5EFjQHPdjjWJAP5Qksn55/view?usp=sharing.

4 Conclusions

This study has illustrated the results of a series of experiments aimed at testing the effectiveness of the optic-flow sensor as a means to perform odometry. In the first test, a single robot moves in an isotropic random walk with and without an object physically attached to its chassis. The results of this test indicate that, the optic-flow and the wheel encoders based odometry are fairly accurate. However, when the object is attached to the robot, the optic-flow sensor outperformed the wheel encoders due to its robustness

to the disruption of the wheel slippage caused by the transport.

In the second test, a multi-robot system engaged in a cooperative transport scenario were evaluated. In this test, the estimate of the linear displacement generated by the optic-flow sensor and the wheel encoder methods have been combined with the estimates of the angular displacement generated by the gyroscope. The results indicate that the optic-flow sensor generates fairly accurate position estimation compared to the wheels encoders. The latter generates position estimates characterised by trajectory lengths longer than the robot's actual trajectories. In addition to the importance of optic-flow sensor in the context of odometry, previous research has shown that in cooperative object transport scenarios, the optic-flow sensor allows a swarm of robots to effectively coordinate their actions and to align individual contributions to transport without the necessity to feel the forces applied to the object (see [Alkilabi et al., 2017]). The sensory information generated by the optic-flow sensors allows the robots to recover from deadlocks and to coordinate their forces in order to avoid working against each other. This study suggests that in order to accurately perform odometry with the optic-flow sensor and gyroscope correction for angular displacement, the best position of the optic-flow sensor is at the robot's centre of mass since, positioned in this way, the optic-flow sensor records no lateral displacements when the robot rotates on the spot. This improves the accuracy of the method by accounting for the lateral displacements in the odometry calculation.

In conclusion, cooperative object transport scenarios are particularly challenging for odometry since frequent wheel slippage and lateral displacement severely disrupt the precision of both the position and orientation estimates. Yet, the results of this research suggest that by using an appropriate sensory apparatus (e.g., optic-flow and gyroscope sensor), odometry can be achieved even in extreme odometry conditions such as those of cooperative object transport scenarios. In future, we plan to develop a cooperative transports scenario in which swarms of robots deliver objects to a target location known by one robot of the group. In this scenario, the robots of a swarm can improve each other localisation estimates by exchanging calculated positions information in order to move the object to a target location.

References

[Alkilabi et al., 2018] Alkilabi, M., Narayan, A., Lu, C., and Tuci, E. (2018). Evolving group transport strategies for e-puck robots: moving objects towards a target area. In et. al., R. G., editor, *Proc. of the Int. Symposium on Distributed Autonomous Robotic Systems (DARS)*. Springer STAR.

[Alkilabi et al., 2017] Alkilabi, M., Narayan, A., and Tuci, E. (2017). Cooperative object transport with a swarm of e-puck robots: robustness and scalability of evolved collective strategies. *Swarm Intelligence*, pages 1–25.

[Borenstein and Feng, 1994] Borenstein, J. and Feng, L. (1994). Umbmark: A method for measuring, comparing, and correcting dead-reckoning errors in mobile robots. *Technical Report UMMEAM-94-22*.

[Dorigo and Şahin, 2004] Dorigo, M. and Şahin, E. (2004). Guest editorial. Special issue: Swarm robotics. *Aut. Rob.*, 17(2–3):111–113.

[Fox et al., 1999] Fox, D., Burgard, W., Kruppa, H., and Thrun, S. (1999). Collaborative multi-robot localization. In *Mustererkennung 1999*, pages 15–26. Springer.

[Gutiérrez et al., 2010] Gutiérrez, A., Campo, A., Monasterio-Huelin, F., Magdalena, L., and Dorigo, M. (2010). Collective decision-making based on social odometry. *Neural Computing and Applications*, 19(6):807–823.

[Kato and Jones, 2013] Kato, S. and Jones, M. (2013). An extended family of circular distributions related to wrapped cauchy distributions via brownian motion. *Bernoulli*, 19(1):154–171.

[Kernbach, 2012] Kernbach, S. (2012). Encoder-free odometric system for autonomous microrobots. *Mechatronics*, 22(6):870–880.

[Kurazume et al., 1994] Kurazume, R., Nagata, S., and Hirose, S. (1994). Cooperative positioning with multiple robots. In *Robotics and Automation, 1994. Proceedings., 1994 IEEE International Conference on*, pages 1250–1257. IEEE.

[Lee and Song, 2004] Lee, S. and Song, J.-B. (2004). Robust mobile robot localization using optical flow sensors and encoders. In *Robotics and Automation, 2004. Proceedings. ICRA'04. 2004 IEEE International Conference on*, volume 1, pages 1039–1044. IEEE.

[Tuci et al., 2018] Tuci, E., Alkilabi, M., and Akanyety, O. (2018). Cooperative object transport in multi-robot systems: A review of the state-of-the-art. *Frontiers in Robotics and AI*, 5:1–15.

[Vardy, 2016] Vardy, A. (2016). Aggregation in robot swarms using odometry. *Artificial Life and Robotics*, 21:443–450.